
Bayesian Optimization for Iterative Learning

Vu Nguyen¹

University of Oxford

Sebastian Schulze¹

University of Oxford

Michael A Osborne

University of Oxford

Abstract

The success of deep (reinforcement) learning systems crucially depends on the correct choice of hyperparameters which are notoriously sensitive and expensive to evaluate. Training these systems typically requires running iterative processes over multiple epochs or episodes. Traditional approaches only consider final performance of a hyperparameter although intermediate information from the learning curve is readily available. In this paper, we present a Bayesian optimization approach which exploits the iterative structure of learning algorithms for efficient hyperparameter tuning. First, we transform each training curve into numeric scores. Second, we selectively augment the data using the information from the curve. This augmentation step enables modeling efficiency while preventing the ill-conditioned issue of Gaussian process covariance matrix if augmenting the whole curve. We demonstrate the efficiency of our algorithm by tuning hyperparameters for the training of deep reinforcement learning agents and convolutional neural networks. Our algorithm outperforms all existing baselines in identifying optimal hyperparameters in minimal time.

1 Introduction

Deep learning (DL) and deep reinforcement learning (DRL) have led to impressive breakthroughs in a broad range of applications such as game play (Mnih et al., 2013; Silver et al., 2016), motor control (Todorov et al., 2012), and image recognition (Krizhevsky et al., 2012). To maintain general applicability, these algorithms expose sets of hyperparameters to adapt their behavior to any particular

task at hand. This flexibility comes at the price of having to tune an additional set of parameters as, particularly in DL and DRL, poor settings lead to drastic performance losses or divergence (Sprague, 2015; Smith, 2018; Henderson et al., 2018). On top of being notoriously sensitive to these choices, deep (reinforcement) learning systems often have high training costs in terms of computational resources and time. For example, a single training iteration on the Atari Breakout game took approximately 75 hours on a GPU cluster (Mnih et al., 2013). Tuning DRL parameters is further complicated as only noisy evaluations of an agent's final performance are obtainable.

Bayesian optimization (BO) (Brochu et al., 2010; Hennig and Schuler, 2012; Shahriari et al., 2016) has recently achieved considerable success in optimizing these hyperparameters. This approach casts the tuning process as a global optimization problem based on noisy evaluations of a black-box function f . BO constructs a surrogate model typically using a Gaussian process (Rasmussen, 2006) over this unknown function. This GP surrogate is used to build an acquisition function (Snoek et al., 2012; Hernández-Lobato et al., 2014; Wang and Jegelka, 2017) which suggests the next hyperparameter to evaluate.

In modern machine learning (ML) algorithms (Jordan and Mitchell, 2015), the training process is typically conducted in an iterative manner. A natural example is given by deep learning where training is often based on stochastic gradient descent and other iterative procedures. Similarly, the training of reinforcement learning agent is mostly carried out using multiple episodes. The knowledge accumulated during these training iterations can be useful to inform Bayesian optimization. However, most of the existing BO approaches (Snoek et al., 2012; Shahriari et al., 2016) define the objective function as the average performance over the final training iterations. In doing so, they ignore the useful information contained in the preceding training steps.

In this paper, we present a Bayesian optimization approach for tuning systems learning iteratively -- the cases of deep learning and deep reinforcement learning. First, we consider the joint space of input hyperparameters and number of training iterations to capture the learning progress at different time steps in the training process. We then

¹These authors contributed equally.

propose to transform the whole training curve into a numeric score according to user preference. To learn across the joint space efficiently, we introduce a data augmentation technique leveraging intermediate information from the iterative process. By exploiting the iterative structure of training procedures, we encourage our algorithm to consider running a larger number of cheap (but high utility) experiments, when cost-ignorant algorithms would only be able to run a few expensive ones. We demonstrate the efficiency of our algorithm on training DRL agents on several well-known benchmarks as well as the training of convolutional neural networks. In particular, our algorithm outperforms existing baselines in finding the best hyperparameter in terms of wall-clock time. Our main contributions are summarized as

- the novel approach to optimizing the learning curve of a ML algorithm by using the training curve compression instead of averaged final performance,
- joint modeling of hyperparameter and iterations with data augmentation for increased sample-efficiency while preventing GP covariance conditioning issues,
- demonstration on tuning DRL and CNNs.

2 Related Work

In the following, we review a number of approaches that aim to minimize the number of training iterations needed to identify the optimal hyperparameters.

The first category employs stopping criteria to terminate some training runs early and instead allocate resources towards more promising settings. These criteria typically evolve around projecting a final score using earlier training stages. Freezethaw BO (Swersky et al., 2014) models the training loss over time using a GP regressor under the assumption that the training loss roughly follows an exponential decay. Based on this projection training resources are allocated to the most promising settings. Hyperband (Li and Jamieson, 2018; Falkner et al., 2018) dynamically allocates the computational resources (e.g., training epochs or dataset size) through random sampling and eliminates under-performing hyperparameter settings by successive halving. In addition, attempts have also been made to improve the epoch efficiency of other hyperparameter optimization algorithms, including (Baker et al., 2017; Domhan et al., 2015; Klein et al., 2017b; Dai et al., 2019) which predict the final learning outcome based on partially trained learning curves to identify hyperparameter settings that are predicted to under-perform and early-stop their model learning. In the context of DRL, however, these stopping criteria may not be applicable due to the unpredictable fluctuations of DRL reward curves. In the supplement, we illustrate the noisiness of DRL training.

The second category (Swersky et al., 2013; Klein et al., 2017a; Kandasamy et al., 2017; Li and Jamieson, 2018) aims to reduce the resource consumption of BO by utilizing low-fidelity functions which can be obtained by using a subset of the training data or by training the ML model for a small number of iterations. Multi-task BO (Swersky et al., 2013) requires the user to define a division of the dataset into pre-defined and discrete subtasks. Multi-fidelity BO with continuous approximation (BOCA) (Kandasamy et al., 2017) extends this idea to continuous settings. Specifically, BOCA first selects the hyperparameter input and then the corresponding fidelity to be evaluated at. The fidelity in this context refers to the use of different number of learning iterations. Analogous to BOCA’s consideration of continuous fidelities, Fabolas (Klein et al., 2017a) proposes to model the joint space of input hyperparameter and dataset size. Then, Fabolas optimizes them jointly to select the optimal input and dataset size.

The above approaches typically identify performance of hyperparameters via the average (either training or validation) loss of the last learning iterations. Thereby, they do not account for potential noise in the learning process (e.g., they might select unstable settings that jump to high performance in the last couple of iterations).

3 Bayesian Optimization for Iterative Learning (BOIL)

We present an efficient hyperparameter optimization algorithm for a machine learning system with iterative learning.

3.1 Problem setting

We consider a machine learning algorithm, which given a d -dimensional hyperparameter $\mathbf{x} \in \mathcal{X} \subset \mathbb{R}^d$, is trained for t iterations. This process has a training time cost $c(\mathbf{x}, t)$ and produces training evaluations $r(\mathbf{x}, t)$ for t iterations, $t \in [T_{\min}, T_{\max}]$. These could be episode rewards in DRL or training accuracies in DL. An important property of iterative training is that we observe the whole curve at preceding steps $r(\mathbf{x}, t')$, $\forall t' \leq t$. We consider the black-box function $f(\mathbf{x}, t)$ mapping from the hyperparameter \mathbf{x} to the score associated with training curve $r(\mathbf{x}, t)$. Formally, we aim to optimize $\mathbf{x}^* = \arg \max_{\mathbf{x} \in \mathcal{X}} f(\mathbf{x}, t)$ at the same time we want to keep the overall training time $\sum_{i=1}^N c(\mathbf{x}_i, t_i)$ of evaluated settings $[\mathbf{x}_i, t_i]$ as low as possible.

3.2 Joint modeling of hyperparameter and iterations

We model the black-box function $f(\mathbf{x}, t)$ as a joint GP where we assume that the objective function at t is a slice of f at t . As a consequence, this GP captures correlations in hyperparameter input and training iteration

$$f(\mathbf{x}, t) \sim GP(0, K([\mathbf{x}, t], [\mathbf{x}', t']))$$

Algorithm 1 Augmenting Data from The Curve

Input: max number of augmented points M , selected input \mathbf{x} , reward curve $r(\mathbf{x}, t)$, threshold δ , data $D_{t,0}$

- 1: **for** $m = 1 \dots M$ **do**
- 2: Select $t' = \arg \max_{u < t} \sigma(\mathbf{x}, u \mid D_{t,m})$
- 3: Break if $\log \text{ of } \text{cond}(K) > \delta$
- 4: Compute y' from $r(\mathbf{x}, t)$ upto t'
- 5: Augment the data $D_{t,m} = D_{t,m-1} \cup (\mathbf{x}, t', y')$.
- 6: **end for**

Output: the augmented data $D_{t,M}$

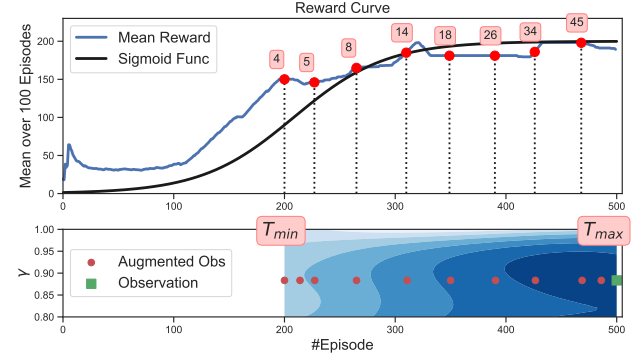


Figure 1: Algorithm description and illustration. The upper plot illustrates an example of training curve and the sigmoid function assigning weight to different training stages for score computation. The lower plot demonstrates which observations are additionally selected to augment the data set.

where $[\mathbf{x}, t] \in \mathcal{R}^{d+1}$ and K is the covariance function. This joint model allows the surrogate to extrapolate across hyperparameter configurations and training iterations. We choose the covariance kernel K as a product $k([\mathbf{x}, t], [\mathbf{x}', t']) = k(\mathbf{x}, \mathbf{x}') \times k(t, t')$. The intuition behind this product kernel is a conjunction of similarities induced by the kernels over parameter and iteration space. We note that similar kernel choices have been used in prior work such as contextual bandits (Krause and Ong, 2011), dynamic BO (Nyikosa et al., 2018), multi-task BO (Swersky et al., 2013), and BO with large datasets (Klein et al., 2017a).

The DRL experiment is notoriously involving noise. In our GP, such noise can be taken into account by the additive i.i.d. Gaussian noise $y_i = f(\mathbf{x}_i) + \varepsilon_i$ where $\varepsilon_i \sim \mathcal{N}(0, \sigma_n^2)$ and σ_n^2 is the noise variance. Under this noise setting, the output follows the GP as $y \sim GP(m, k + \sigma_n^2 \delta_{i,j})$ where $\delta_{i,j} = 1$ iff $i = j$ is the Kronecker's delta.

Based on the above surrogate function, we can estimate the predictive mean and uncertainty of a Gaussian process for any input $\mathbf{z}_* = [\mathbf{x}_*, t_*]$ (Rasmussen, 2006) as

$$\mu(\mathbf{z}_*) = \mathbf{k}_* [\mathbf{K} + \sigma_n^2 \delta_{i,j}]^{-1} \mathbf{y} \quad (1)$$

$$\sigma^2(\mathbf{z}_*) = k_{**} - \mathbf{k}_* [\mathbf{K} + \sigma_n^2 \delta_{i,j}]^{-1} \mathbf{k}_*^T \quad (2)$$

where $k_{**} = k(\mathbf{z}_*, \mathbf{z}_*)$, $\mathbf{k}_* = [k(\mathbf{z}_*, \mathbf{z}_i)]_{\forall i \leq N}$ and $\mathbf{K} = [k(\mathbf{z}_i, \mathbf{z}_j)]_{\forall i, j \leq N}$. These estimates are useful to compute the acquisition function. To cope with output noise, we follow (Wang and de Freitas, 2014) to use a slight modification of the incumbent as μ_n^{\max} which is the maximum of GP mean. Let $\lambda = \frac{\mu_n(\mathbf{z}) - \mu_n^{\max}}{\sigma_n(\mathbf{z})}$, we then have a closed-form

$$\alpha_n^{\text{EI}}(\mathbf{z}) = \sigma_n(\mathbf{z}) \phi(\lambda) + [\mu_n(\mathbf{z}) - \mu_n^{\max}] \Phi(\lambda) \quad (3)$$

where ϕ is the standard normal p.d.f. and Φ is the c.d.f. We note that our framework is readily available for any other acquisition choices (Hennig and Schuler, 2012; Hernández-Lobato et al., 2014; Wu and Frazier, 2016; Letham et al., 2019).

Surrogate cost model. We consider the cost function $\tau(\mathbf{x}, t)$, where the cost observation is denoted as $c(\mathbf{x}, t)$, as the training time and build an additional GP surrogate model for the expected training cost (time) as a function of hyperparameter-iteration pairs $[\mathbf{x}, t] \in \mathcal{X} \times \mathcal{R}$. The analytical formula for this GP is similar to Eq. (1) and Eq. (2), except the output y is now the training time $c(\mathbf{x}, t)$.

3.3 Training curve compression

Existing BO approaches (Chen et al., 2018; Li and Jamieson, 2018) typically define the objective function as an average loss over the final learning episodes. However, this does not take into consideration how stable performance is or the training stage at which it has been achieved. In our model, averaging learning losses is likely to be misleading due to the noise of our observations -- particularly during the early stages of training. We suggest to compress the whole learning curve into a numeric score via a preference function representing the user's desired training curve -- in the following we use the Sigmoid function. Given the training curve, we compute the utility score as

$$y = \sum_{i=1}^t r(i) \times l(i) \quad (4) \quad l(x) = \frac{1}{1 + \exp(-x)} \quad (5)$$

Note that more generally, $l(i)$ can depend on the length t of the training curve and for appropriate choices, i.e. $l(i) = \frac{1}{t}, \forall i$, we recover the averaging described above. The Sigmoid preference has a number of desirable properties. As the early weights are small, less credit is given to fluctuations at the initial stages, making it less likely for our surrogate to be biased towards randomly well performing settings. However, as weights monotonically increase, hyperparameters enabling learning (and therefore improved performance) are preferred. As weights saturate over time, stable, high performing configurations is preferred over short "performance spikes" characteristic of unstable training.

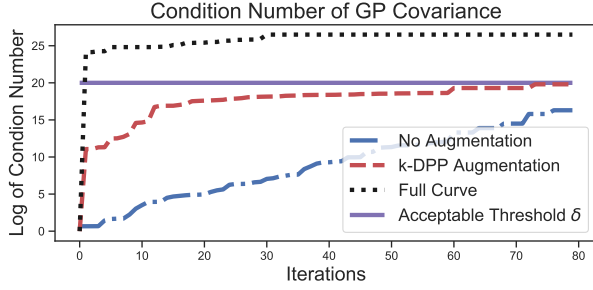


Figure 2: The condition number of GP covariance matrix goes badly if we add noisy observations closely each other. The large condition number measures the nearness to singularity. This happens when we add the whole curve of points into a GP.

Lastly, this utility score assigns higher values to the same performance if it is being maintained over more episodes. We illustrate the reward transformation using the Sigmoid function in Fig. 1. In Fig. 10 in the appendix, we further demonstrate that our model is robust with different preference choices.

3.4 Augmenting data with intermediate observations

When evaluating a configuration \mathbf{x} for a number of iterations t , we obtain not only a final score but also all reward sequences $r(\mathbf{x}, t')$, $\forall t' = 1, \dots, t$. The auxiliary information from the curve can bring useful information for Bayesian optimization. Therefore, we propose to augment the sample set of our GP model using the information from the curve. This prevents the algorithm from reselecting the same input \mathbf{x} at the lower fidelity (e.g., lower training iteration) $t' < t$ by reducing uncertainty around these locations. This uncertainty reduction lowers the value of the acquisition function and encourages exploration elsewhere.

Ill-conditioned issue with augmenting a full curve. A naive approach for augmentation is to add a full curve of points $\{[\mathbf{x}, j], y_j\}_{j=1}^t$ where y_j is computed from $r(\mathbf{x}, j)$ using Eq. (4). However, this approach impose serious issues in conditioning of the GP covariance matrix. As we cluster more evaluations closely, the conditioning of the GP covariance degrades further, as discussed in (McLeod et al., 2018). This conditioning issue is especially serious in our DRL noisy curve fluctuating widely. We highlight this negative effect in Fig. 2 where the *log* of condition number goes above 25 if we augment the whole curve. Then, we illustrate the effect on GP estimation in Fig. 3 wherein the GP mean estimation goes off significantly large and small in the bottom row due to the undesirable effect of the GP covariance condition number.

Therefore, it is essential to selectively augment the observations from the learning curve. While it is not triv-

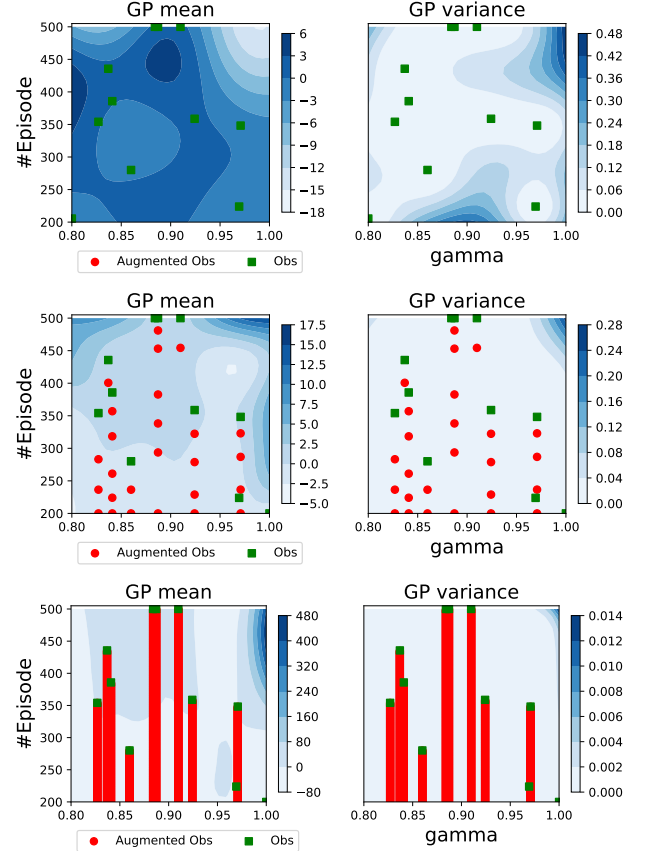


Figure 3: GP with different settings of augmentation. Top: No augmentation. Middle: the proposed augmentation. Bottom: using a full curve. By adding more observations, the GP uncertainty reduces (right column). However, if we add too much observations (bottom row), the GP covariance matrix becomes ill-conditioned, thus the GP mean estimation could be inaccurately estimated (bottom left).

ial to intervene the condition number of the GP covariance, we can mitigate such conditioning issue by discouraging adding similar points closely each other, as shown in (McLeod et al., 2018). Among the existing active learning approaches (Osborne et al., 2012; Contal et al., 2013; Gal et al., 2017), we utilize a determinantal point process (Kulesza et al., 2012) which will relax to maximizing a GP variance under a greedy setting.

k-DPP for selecting most informative points. By an abuse of notation, we use M -DPP to represent k -DPP since k is the kernel in our context. Given a training curve $r(\mathbf{x}, t_i)$ and conditioning on the inclusion of an existing observations D_n , we want to find a diverse set $[t_1, \dots, t_M], \forall t_m \leq t$ to augmented into \mathbf{x} to form additional observations $Z = [z_1, \dots, z_M]$ where each $z_m = [\mathbf{x}, t_m]$,

$$p^M(D \cup Z | D) \propto \det(K_Z - K_{ZD}K_D^{-1}K_{DZ}). \quad (6)$$

While the discrete-DPP sampler formally extends to the

Algorithm 2 Bayes Opt with Iterative Learning (BOIL)

Input: #iter N , initial data D_0 , define $\mathbf{z} = [\mathbf{x}, t]$

- 1: **for** $n = 1 \dots N$ **do**
 - 2: Fit a GP and acquisition function $\alpha(\mathbf{x}, t)$ from the joint space of parameter-iteration
 - 3: Fit a surrogate model for cost function $\tau(\mathbf{x}, t)$
 - 4: Select $\mathbf{z}_n = \arg \max_{\mathbf{x}, t} \alpha(\mathbf{x}, t) / \tau(\mathbf{x}, t)$
 - 5: Observe $r_n, c_n = f(\mathbf{z}_n)$ # r_n is a training curve, c_n is a cost (i.e., training time)
 - 6: Compute y_n from the curve r_n using Eq. (4)
 - 7: Augment observations $\mathbf{z}_{n,m}, y_{n,m}, c_{n,m}, \forall m \leq M$ given r_n and D_t in Alg. 1
 - 8: $D_n = D_{n-1} \cup (\mathbf{z}_n, y_n, c_n) \cup (\mathbf{z}_{n,m}, y_{n,m}, c_{n,m})$.
 - 9: **end for**
- Output: optimal \mathbf{x}^* and $y^* = \max_{\mathbf{y} \in D_N} y$
-

continuous case, the required computation is not tractable in general. In practice, we utilize greedy approximations by sequentially selecting points to create a batch of M points (Kathuria et al., 2016). The M -DPP reduces to M sequential draws from 1-DPPs in each of which the determinant computation in Eq. (6) reduces to a scalar equivalent to a GPs predictive variance in Eq. (2). This relaxation . Formally, we sequentially select a set $Z = [z_1, \dots, z_M]$ by varying t_m while keeping \mathbf{x} fixed as

$$z_m = \arg \max_{\forall t' \leq t} k_{z'} - \mathbf{k}_{z'} D' \mathbf{K}_{D'}^{-1} \mathbf{k}_{D', z'} = \arg \max_{\forall t' \leq t} \sigma(t' | D') \quad (7)$$

where $z_m = [\mathbf{x}, t_m]$ and $D' = D \cup \{z_j = [\mathbf{x}, t_j]\}_{j=1}^{m-1}$.

Estimating scores for augmented observations. For each augmented point $[\mathbf{x}, t_m]$, we compute the utility score y_m for this point from Eq. (4) by cropping the initial training curve $r(\mathbf{x}, t)$ to $r(\mathbf{x}, t_m)$ since $t_m \leq t$. In addition, we can either observe or interpolate the running time cost c_m at this augmented observation (\mathbf{x}, t_m) . Finally, at each iteration n of the main BO algorithm, we obtain a collection of upto M augmented points including $\mathbf{z}_{n,m}, y_{n,m}, c_{n,m}, \forall m \leq M$ where $\mathbf{z}_{n,m} = [\mathbf{x}_{n,m}, t_{n,m}]$. In practice, we use a threshold δ to terminate the augmentation step if the log of GP covariance condition number exceeds δ . This is to ensure that the GP covariance matrix condition number behaves well by reducing the number of unnecessary points added to the GP at later stages. We refer to Fig. 1 for the illustration on the augmented observations and estimated scores.

3.5 Algorithm

To enforce non-negativity and numerical stability in the utility α and cost functions τ , we make use of the transformations $\alpha = \log(1 + \exp(\alpha))$ and $\tau = \log(1 + \exp(\tau))$. At each iteration n , we query the input parameter \mathbf{x}_n and

the number of iteration t_n :

$$\mathbf{z}_n = [\mathbf{x}_n, t_n] = \arg \max_{\mathbf{x} \in \mathcal{X}, t \in [T_{\min}, T_{\max}]} \alpha(\mathbf{x}, t) / \tau(\mathbf{x}, t). \quad (8)$$

By evaluating the black-box function, we obtain the training curve r_n and the training time c_n . Using this information, we generate up to M augmented observations $\mathbf{z}_{n,m}, y_{n,m}, c_{n,m}, \forall m \leq M$ from the new point \mathbf{z}_n and add them into our dataset D_n . We summarize our approach in Alg. 2.

4 Experiments

We demonstrate our proposed model by tuning hyperparameters for several deep reinforcement learning agents and convolutional neural networks (CNN). We provide additional illustrations and experiments in the supplement.

4.1 Experimental setup and baselines

All experimental results described below are averaged over 20 independently performed runs with different random seeds. Unless otherwise indicated, final performance is estimated by evaluating the chosen hyperparameter over the maximum number of iterations. All experiments are executed on a NVIDIA 1080 GTX GPU using the tensorflow-gpu Python package. The DRL environments are available through the OpenAI gym (Brockman et al., 2016) and Mujoco (Todorov et al., 2012). Our DRL implementations are based on the open source from Open AI Baselines (Dhariwal et al., 2017). We will release all source codes and packages in the final version.

We use square-exponential kernels for the GPs in our model and estimate their parameters using maximum marginal likelihood (Rasmussen, 2006). In Alg. 1, we set maximum the number of augmented points $M = 15$ and a threshold for log of GP covariance condition number is $\delta = 20$. We note that the optimization overhead is much less than the function evaluation time. In particular, the data augmentation step takes only 1% the time used for each DRL evaluation.

We select to compare with Hyperband (Li and Jamieson, 2018) which demonstrates empirical successes in tuning deep learning applications in an iteration-efficient manner. We extend the discrete (Swersky et al., 2013) to the continuous multi-task BO (or CMTBO) -- which can be seen as our BOIL without augmentation. We do not compare with Fabolas (Klein et al., 2017a) because Fabolas is designed for varying dataset sizes, not iteration axis. We omit to compare with BOCA (Kandasamy et al., 2017) because the source code is not available and the algorithm specification is not trivial to re-implement. We also expect the performance of (Kandasamy et al., 2017) to be close (if not inferior) to CMTBO. This is because CMTBO jointly optimizes the fidelity and input while BOCA first selects the

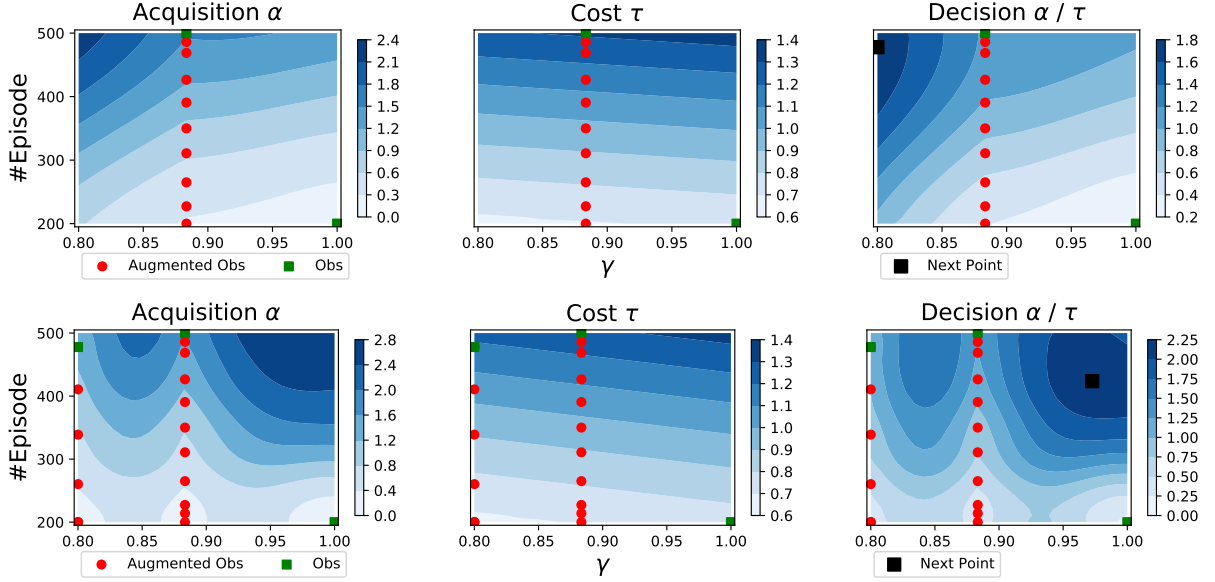


Figure 4: Illustration of model behavior in two consecutive evaluations on a 2-dimensional optimization task of tuning DDQN on CartPole. Our model selects a point (black square) by balancing the cost function and the value function.

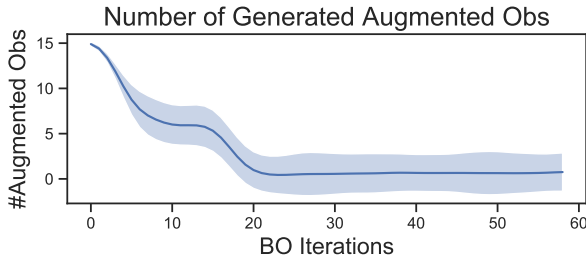


Figure 5: DDQN on CartPole. Number of augmented observations added to the data set is reducing over time.

input and then the fidelity. To demonstrate the impact of our training curve compression we also compare BOIL to vanilla Bayesian optimization for which we fix the number of iterations at T_{max} . Here, we consider two different objective functions - the averaged performance over the final 100 training iterations (BO) and our compressed score (BO-L).

4.2 Model behavior illustration

We show our algorithm’s behavior over two iterations in Fig. 4. The decision function balances utility score encoded in the acquisition function α and cost τ to make an iteration-efficient choice. The red dots are the augmented observations generated to learn our joint space of hyperparameter-episode faster. As seen in Fig. 4, queries are chosen at locations of high utility. When presented with several locations of similar value, BOIL makes the iteration-efficient choice of evaluating points with lower cost. We provide further illustrations in the supplement.

We next examine the count of augmented observations generated per iteration in Fig. 5. Although this number is fluctuating, it tends to reduce over time. BOIL does not add more augmented observations at the later stage when we have gained sufficient information and GP covariance conditioning falls below our threshold δ .

4.3 Tuning deep reinforcement learning and CNN

We now optimize hyperparameters for deep reinforcement learning algorithms; in fact, this application motivated the development of BOIL. The combinations of hyperparameters to be tuned, target DRL algorithm and environment are detailed below. Additional information about these settings including parameter ranges can be found in the supplement.

Task descriptions. We consider three DRL settings to demonstrate BOIL’s ability to optimize highly noisy objectives. In the first, we optimize learning rate α and discount factor γ of a Dueling DQN (DDQN) (Wang et al., 2016) agent in the CartPole-v0 environment. In the last two, we optimize actor learning rate α_1 , critic learning rate α_2 and discount factor γ of Advantage Actor Critic (A2C) (Mnih et al., 2016) agents in the InvertedPendulum-v2 and Reacher-v2 environments. In all cases, the learning rates are part of Adam optimizers (Kingma and Ba, 2014) and we use the standard length of 200 steps per episode. Due to space considerations, we present the plots of the DDQN-Cartpole setting in the supplement and also refer to the supplement for further experimental details.

In addition to the DRL applications, we tune 6 hyperparameters for training a convolutional neural network (Le-

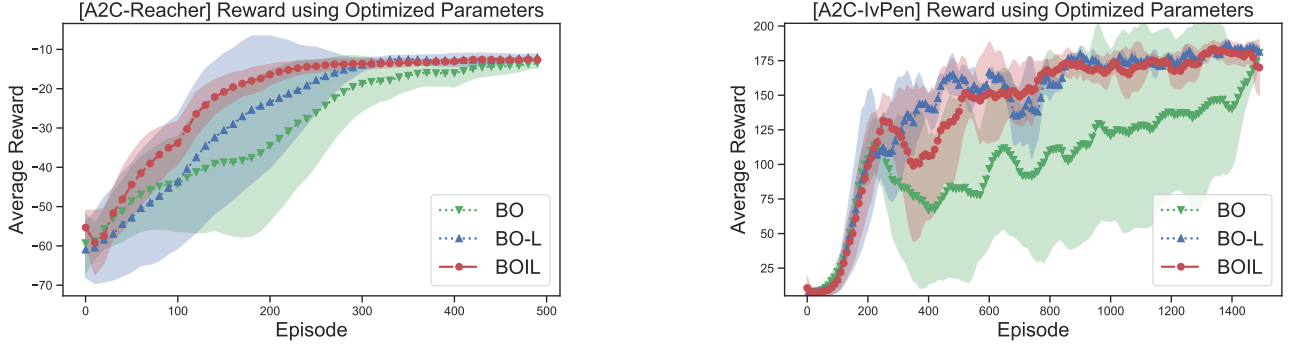


Figure 6: The plots illustrate the learning curves of the best found parameters identified by different approaches. The curves show that BO-L and BOIL reliably identify parameters leading to stable training. BOIL takes only half total time to find this optimal curve. Without considering the whole curve, BO can only identify sub-optimal hyperparameters.

Cun et al., 1998) on the SVHN dataset (Netzer et al., 2011) as summarized in Table 1c in the supplement. We use two CNN layers, two fully connected layers and RMSProp (Hinton et al., 2012) as the main optimizer. The dataset is divided into 10,000 training images and a held-out test set of 10,000 images for evaluation. Optimizing 6 hyperparameters demonstrates the scalability of our approach.

Comparison of final learning curves. We first demonstrate the improvement in stability gained by using the proposed learning curve compression. For this, we examine the learning curves of the best hyperparameters identified by BO, BO-L and BOIL. Fig. 6 shows the learning progress over T_{\max} episodes for each of these. The curves are smoothed by averaging over 100 consecutive episodes for increased clarity. We first note, that all three algorithms eventually obtain similar performance at the end of learning. However, since BO-L and BOIL take into account the preceding learning steps, they achieve higher performance more quickly. Furthermore, they achieve this more reliably as evidenced by the smaller error bars (shaded regions).

Performance comparisons across iterations and real-time. Fig. 7 plots the performance of different algorithms against the number of iterations as well as real-time. The performance is the utility score of the best hyperparameters identified by the baselines. Across all three tasks, BOIL identifies optimal hyperparameters using significantly less computation time than other approaches.

The plots show that other approaches such as BO and BO-L can identify well-performing hyperparameters in fewer iterations than BOIL. However, they do so only considering costly, high-fidelity evaluations resulting in significantly higher evaluation times. In contrast to this behavior, BOIL accounts for the evaluation costs and chooses to initially evaluate low-fidelity settings consuming less time. This allows fast assessments of a multitude of hyperparameters. The information gathered here is then used to inform later

point acquisitions. Hereby, the inclusion of augmented observations is crucial as it prevents the algorithm to reselect the input parameter \mathbf{x} at lower fidelity t' if \mathbf{x} has been evaluated at higher fidelity $t > t'$. In addition, this augmentation is essential to prevent from the GP kernel issue instead of adding the full curve of points into our GP model.

Hyperband (Li and Jamieson, 2018) exhibits similar behavior in that it uses low fidelity (small t) evaluations to reduce a pool of randomly sampled configurations before evaluating at high fidelity (large t). To hedge against noisy evaluations and other effects, this process is repeated several times. This puts Hyperband at a disadvantage particularly in the noisy DRL tasks. Since early performance fluctuates hugely, Hyperband can be misled in where to allocate evaluation effort. It is then incapable of revising these choices until an entirely pool of hyperparameters is sampled and evaluated from scratch. In contrast to this, BOIL is more flexible than Hyperband in that it can freely explore-exploit the whole joint space. The GP surrogate hereby allows BOIL to generalize across hyperparameters and propagate information through the joint space.

5 Conclusion and Future work

Our framework complements the existing BO toolbox for hyperparameter tuning with iterative learning. We present a way of leveraging our understanding that later stages of the training process are informed by progress made in earlier ones. This results in a more iteration-efficient hyperparameter tuning algorithm that is applicable to a broad range of machine learning systems. We evaluate its performance on a set of diverse benchmarks. The results demonstrate that our model can surpass the performance of well-established alternatives while consuming significantly fewer resources. Finally, we would like to note that our approach is not necessarily specific to machine learning algorithms but more generally applies to any process exhibiting an iterative structure to be exploited.

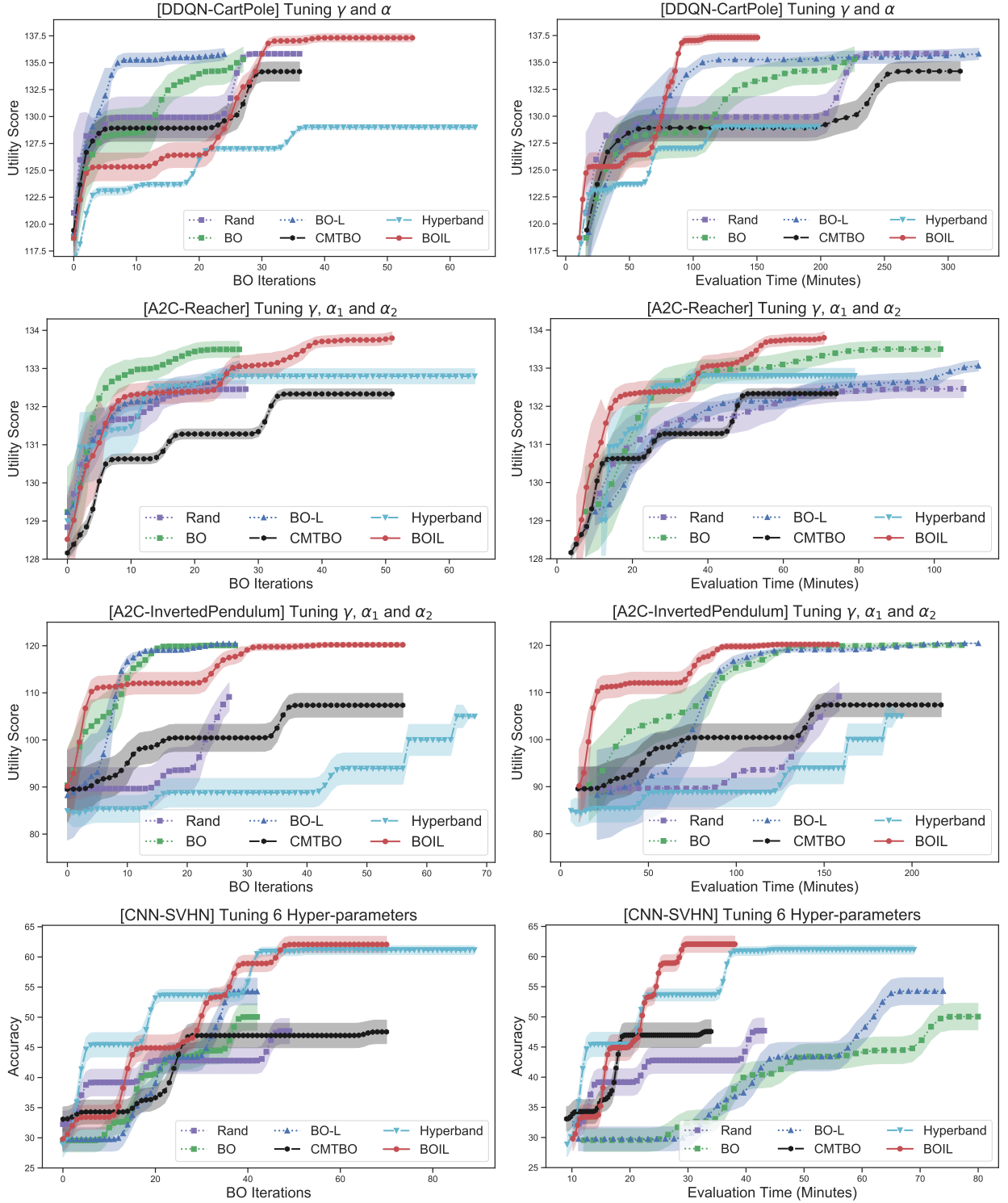


Figure 7: Comparison of performance over BO evaluations (Left) and real-time (Right). Given the same time budget, CMTBO, Hyperband and BOIL can take more evaluations than vanilla BO, BO-L and Rand. BOIL outperforms other competitors in finding the optimal parameters in an iteration-efficient manner. BOIL exploits the knowledge about the training curve by selectively augmenting the data for GP with informative observations. CMTBO is less efficient comparing to BOIL. CMTBO does not augment the observations from the curve that CMTBO requires more evaluations and it can unnecessarily reselect parameters at lower fidelity.

References

- Bowen Baker, Otkrist Gupta, Ramesh Raskar, and Nikhil Naik. Accelerating neural architecture search using performance prediction. *arXiv preprint arXiv:1705.10823*, 2017.
- Eric Brochu, Vlad M Cora, and Nando De Freitas. A tutorial on bayesian optimization of expensive cost functions, with application to active user modeling and hierarchical reinforcement learning. *arXiv preprint arXiv:1012.2599*, 2010.
- Greg Brockman, Vicki Cheung, Ludwig Pettersson, Jonas Schneider, John Schulman, Jie Tang, and Wojciech Zaremba. Openai gym. *arXiv preprint arXiv:1606.01540*, 2016.
- Yutian Chen, Aja Huang, Ziyu Wang, Ioannis Antonoglou, Julian Schrittwieser, David Silver, and Nando de Freitas. Bayesian optimization in alphago. *arXiv preprint arXiv:1812.06855*, 2018.
- Emile Contal, David Buffoni, Alexandre Robicquet, and Nicolas Vayatis. Parallel gaussian process optimization with upper confidence bound and pure exploration. In *Machine Learning and Knowledge Discovery in Databases*, pages 225–240. Springer, 2013.
- Zhongxiang Dai, Haibin Yu, Bryan Kian Hsiang Low, and Patrick Jaillet. Bayesian optimization meets bayesian optimal stopping. In *International Conference on Machine Learning*, pages 1496–1506, 2019.
- Prafulla Dhariwal, Christopher Hesse, Oleg Klimov, Alex Nichol, Matthias Plappert, Alec Radford, John Schulman, Szymon Sidor, Yuhuai Wu, and Peter Zhokhov. Openai baselines. *GitHub, GitHub repository*, 2017.
- Tobias Domhan, Jost Tobias Springenberg, and Frank Hutter. Speeding up automatic hyperparameter optimization of deep neural networks by extrapolation of learning curves. In *Twenty-Fourth International Joint Conference on Artificial Intelligence*, 2015.
- Stefan Falkner, Aaron Klein, and Frank Hutter. Bohb: Robust and efficient hyperparameter optimization at scale. In *International Conference on Machine Learning*, pages 1436–1445, 2018.
- Peter I Frazier. A tutorial on bayesian optimization. *arXiv preprint arXiv:1807.02811*, 2018.
- Yarin Gal, Riashat Islam, and Zoubin Ghahramani. Deep bayesian active learning with image data. In *Proceedings of the 34th International Conference on Machine Learning*, pages 1183–1192. JMLR. org, 2017.
- Peter Henderson, Riashat Islam, Philip Bachman, Joelle Pineau, Doina Precup, and David Meger. Deep reinforcement learning that matters. In *Thirty-Second AAAI Conference on Artificial Intelligence*, 2018.
- Philipp Hennig and Christian J Schuler. Entropy search for information-efficient global optimization. *Journal of Machine Learning Research*, 13:1809–1837, 2012.
- José Miguel Hernández-Lobato, Matthew W Hoffman, and Zoubin Ghahramani. Predictive entropy search for efficient global optimization of black-box functions. In *Advances in Neural Information Processing Systems*, pages 918–926, 2014.
- Geoffrey Hinton, Nitish Srivastava, and Kevin Swersky. Overview of mini-batch gradient descent. *Neural Networks for Machine Learning*, 575, 2012.
- M. I. Jordan and T. M. Mitchell. Machine learning: Trends, perspectives, and prospects. *Science*, 349(6245): 255–260, 2015. doi: 10.1126/science.aaa8415.
- Kirthevasan Kandasamy, Gautam Dasarathy, Jeff Schneider, and Barnabás Póczos. Multi-fidelity bayesian optimisation with continuous approximations. In *Proceedings of the 34th International Conference on Machine Learning—Volume 70*, pages 1799–1808. JMLR.org, 2017.
- Tarun Kathuria, Amit Deshpande, and Pushmeet Kohli. Batched gaussian process bandit optimization via determinantal point processes. In *Advances in Neural Information Processing Systems*, pages 4206–4214, 2016.
- Diederik P Kingma and Jimmy Ba. Adam: A method for stochastic optimization. *arXiv preprint arXiv:1412.6980*, 2014.
- Aaron Klein, Stefan Falkner, Simon Bartels, Philipp Hennig, and Frank Hutter. Fast bayesian optimization of machine learning hyperparameters on large datasets. In *Artificial Intelligence and Statistics*, pages 528–536, 2017a.
- Aaron Klein, Stefan Falkner, Jost Tobias Springenberg, and Frank Hutter. Learning curve prediction with bayesian neural networks. *International Conference on Learning Representations (ICLR)*, 2017b.
- Andreas Krause and Cheng S Ong. Contextual gaussian process bandit optimization. In *Advances in Neural Information Processing Systems*, pages 2447–2455, 2011.
- Alex Krizhevsky, Ilya Sutskever, and Geoffrey E Hinton. Imagenet classification with deep convolutional neural networks. In *Advances in neural information processing systems*, pages 1097–1105, 2012.
- Alex Kulesza, Ben Taskar, et al. Determinantal point processes for machine learning. *Foundations and Trends® in Machine Learning*, 5(2–3):123–286, 2012.

- Yann LeCun, Léon Bottou, Yoshua Bengio, and Patrick Haffner. Gradient-based learning applied to document recognition. *Proceedings of the IEEE*, 86(11):2278–2324, 1998.
- Benjamin Letham, Brian Karrer, Guilherme Ottoni, Eytan Bakshy, et al. Constrained bayesian optimization with noisy experiments. *Bayesian Analysis*, 14(2):495–519, 2019.
- Lisha Li and Kevin Jamieson. Hyperband: A novel bandit-based approach to hyperparameter optimization. *Journal of Machine Learning Research*, 18:1–52, 2018.
- Mark McLeod, Stephen Roberts, and Michael A Osborne. Optimization, fast and slow: Optimally switching between local and bayesian optimization. In *International Conference on Machine Learning*, pages 3440–3449, 2018.
- Volodymyr Mnih, Koray Kavukcuoglu, David Silver, Alex Graves, Ioannis Antonoglou, Daan Wierstra, and Martin Riedmiller. Playing atari with deep reinforcement learning. *arXiv preprint arXiv:1312.5602*, 2013.
- Volodymyr Mnih, Adria Puigdomenech Badia, Mehdi Mirza, Alex Graves, Timothy Lillicrap, Tim Harley, David Silver, and Koray Kavukcuoglu. Asynchronous methods for deep reinforcement learning. In *International conference on machine learning*, pages 1928–1937, 2016.
- Yuval Netzer, Tao Wang, Adam Coates, Alessandro Bisaccho, Bo Wu, and Andrew Y Ng. Reading digits in natural images with unsupervised feature learning. 2011.
- Favour M Nyikosa, Michael A Osborne, and Stephen J Roberts. Bayesian optimization for dynamic problems. *arXiv preprint arXiv:1803.03432*, 2018.
- Michael Osborne, Roman Garnett, Zoubin Ghahramani, David K Duvenaud, Stephen J Roberts, and Carl E Rasmussen. Active learning of model evidence using bayesian quadrature. In *Advances in neural information processing systems*, pages 46–54, 2012.
- Carl Edward Rasmussen. Gaussian processes for machine learning. 2006.
- Tom Schaul, John Quan, Ioannis Antonoglou, and David Silver. Prioritized experience replay. *International Conference on Learning Representations*, 2016.
- Bobak Shahriari, Kevin Swersky, Ziyu Wang, Ryan P Adams, and Nando de Freitas. Taking the human out of the loop: A review of Bayesian optimization. *Proceedings of the IEEE*, 104(1):148–175, 2016.
- David Silver, Aja Huang, Chris J Maddison, Arthur Guez, Laurent Sifre, George Van Den Driessche, Julian Schrittwieser, Ioannis Antonoglou, Veda Panneershelvam, Marc Lanctot, et al. Mastering the game of go with deep neural networks and tree search. *Nature*, 529(7587):484, 2016.
- Leslie N Smith. A disciplined approach to neural network hyper-parameters: Part 1—learning rate, batch size, momentum, and weight decay. *arXiv preprint arXiv:1803.09820*, 2018.
- Jasper Snoek, Hugo Larochelle, and Ryan P Adams. Practical Bayesian optimization of machine learning algorithms. In *Advances in neural information processing systems*, pages 2951–2959, 2012.
- Nathan Sprague. Parameter selection for the deep q-learning algorithm. In *Proceedings of the Multidisciplinary Conference on Reinforcement Learning and Decision Making (RLDM)*, page 24, 2015.
- Kevin Swersky, Jasper Snoek, and Ryan P Adams. Multi-task Bayesian optimization. In *Advances in neural information processing systems*, pages 2004–2012, 2013.
- Kevin Swersky, Jasper Snoek, and Ryan Prescott Adams. Freeze-thaw bayesian optimization. *arXiv preprint arXiv:1406.3896*, 2014.
- Emanuel Todorov, Tom Erez, and Yuval Tassa. Mujoco: A physics engine for model-based control. In *2012 IEEE/RSJ International Conference on Intelligent Robots and Systems*, pages 5026–5033. IEEE, 2012.
- Zi Wang and Stefanie Jegelka. Max-value entropy search for efficient bayesian optimization. In *International Conference on Machine Learning*, pages 3627–3635, 2017.
- Ziyu Wang and Nando de Freitas. Theoretical analysis of bayesian optimisation with unknown gaussian process hyper-parameters. *arXiv preprint arXiv:1406.7758*, 2014.
- Ziyu Wang, Tom Schaul, Matteo Hessel, Hado Hasselt, Marc Lanctot, and Nando Freitas. Dueling network architectures for deep reinforcement learning. In *International Conference on Machine Learning*, pages 1995–2003, 2016.
- Jian Wu and Peter Frazier. The parallel knowledge gradient method for batch Bayesian optimization. In *Advances In Neural Information Processing Systems*, pages 3126–3134, 2016.

Appendix

We provide the readers further insights into our design choices and a deeper understanding of the algorithms properties. First, we give a brief overview of Bayesian optimization with Gaussian processes. We then illustrate our models behavior on a two dimensional problem. Last, we give further details of our experiments for reproducibility purposes.

A Bayesian Optimization Preliminaries

Bayesian optimization is a sequential approach to global optimization of black-box functions without making use of derivatives. It uses two components: a learned surrogate model of the objective function and an acquisition function derived from the surrogate for selecting new points to inform the surrogate with. In-depth discussions beyond our brief overview can be found in recent surveys (Brochu et al., 2010; Shahriari et al., 2016; Frazier, 2018).

A.1 Gaussian processes

The most common choice of surrogate models is the Gaussian process (GP) (Rasmussen, 2006). A GP defines a probability distribution over functions f under the assumption that any subset of point $\{(\mathbf{x}_i, f(\mathbf{x}_i))\}$ is normally distributed. Formally, this is denoted as:

$$f(\mathbf{x}) \sim GP(m(\mathbf{x}), k(\mathbf{x}, \mathbf{x}'))$$

where $m(\mathbf{x})$ and $k(\mathbf{x}, \mathbf{x}')$ are the mean and covariance functions, given by $m(\mathbf{x}) = \mathbb{E}[f(\mathbf{x})]$ and $k(\mathbf{x}, \mathbf{x}') = \mathbb{E}[(f(\mathbf{x}) - m(\mathbf{x}))(f(\mathbf{x}') - m(\mathbf{x}'))^T]$.

Typically, the mean of GP is assumed to be zero everywhere. The kernel $k(\mathbf{x}, \mathbf{x}')$ can be thought of as a similarity measure relating $f(\mathbf{x})$ and $f(\mathbf{x}')$. Numerous kernels encoding different prior beliefs about $f(\mathbf{x})$ have been proposed. A popular choice is given by the square exponential kernel $k(\mathbf{x}, \mathbf{x}') = \sigma_f^2 \exp[-(\mathbf{x} - \mathbf{x}')^2 / 2\sigma_f^2]$. The length-scale σ_f^2 regulates the maximal covariance between two points and can be estimated using maximum marginal likelihood. The SE kernel encodes the belief that nearby points are highly correlated as it is maximized at $k(\mathbf{x}, \mathbf{x}') = \sigma_f^2$ and decays the further \mathbf{x} and \mathbf{x}' are separated.

For prediction at a new data point \mathbf{x}_* , let denote $f_* = f(\mathbf{x}_*)$ we have

$$\begin{bmatrix} f \\ f_* \end{bmatrix} \sim \mathcal{N}\left(0, \begin{bmatrix} K & \mathbf{k}_*^T \\ \mathbf{k}_* & k_{**} \end{bmatrix}\right) \quad (9)$$

where $k_{**} = k(\mathbf{x}_*, \mathbf{x}_*)$, $\mathbf{k}_* = [k(\mathbf{x}_*, \mathbf{x}_i)]_{\forall i \leq N}$ and $K = [k(\mathbf{x}_i, \mathbf{x}_j)]_{\forall i, j \leq N}$. The conditional probability of $p(f_* | f)$ follows a univariate Gaussian distribution as $p(f_* | f) \sim$

$\mathcal{N}(\mu(\mathbf{x}_*), \sigma^2(\mathbf{x}_*))$. Its mean and variance are given by

$$\begin{aligned} \mu(\mathbf{x}_*) &= \mathbf{k}_* [\mathbf{K} + \sigma_n^2 \delta_{i,j}]^{-1} \mathbf{y} \\ \sigma^2(\mathbf{x}_*) &= k_{**} - \mathbf{k}_* [\mathbf{K} + \sigma_n^2 \delta_{i,j}]^{-1} \mathbf{k}_*^T \end{aligned}$$

where σ_n^2 is the output noise variance. As GPs give full uncertainty information with any prediction, they provide a flexible non-parametric prior for Bayesian optimization. We refer the interested readers to (Rasmussen, 2006) for further details in Gaussian process.

A.2 Acquisition function

Bayesian optimization is typically applied in settings in which the objective function is expensive to evaluate. To minimize interactions with that objective, an acquisition function is defined to reason about the selection of the next evaluation point $\mathbf{x}_{t+1} = \arg \max_{\mathbf{x} \in \mathcal{X}} \alpha_t(\mathbf{x})$. The acquisition function is constructed from the predictive mean and variance of the surrogate to be easy to evaluate and represents the trade-off between exploration (of points with high predictive uncertainty) and exploitation (of points with high predictive mean). Thus, by design the acquisition function can be maximized with standard global optimization toolboxes.

A.3 GP kernels and treatment of GP hyperparameters

Although the raw learning curve in DRL is noisy, the transformed version using our proposed curve compression makes the resulting curve smooth. Therefore, we use the two squared exponential kernels for input hyperparameter and training iteration, respectively. That is $k_x(\mathbf{x}, \mathbf{x}') = \exp\left(-\frac{\|\mathbf{x} - \mathbf{x}'\|^2}{2\sigma_x^2}\right)$ and $k_t(t, t') = \exp\left(-\frac{\|t - t'\|^2}{2\sigma_t^2}\right)$ where the observation \mathbf{x} and t are normalized to $[0, 1]^d$ and the outcome y is standardized $y \sim \mathcal{N}(0, 1)$ for robustness. As a result, our product kernel becomes

$$\begin{aligned} k([\mathbf{x}, t], [\mathbf{x}', t']) &= k(\mathbf{x}, \mathbf{x}') \times k(t, t') \\ &= \exp\left(-\frac{\|\mathbf{x} - \mathbf{x}'\|^2}{2\sigma_x^2} - \frac{\|t - t'\|^2}{2\sigma_t^2}\right). \end{aligned}$$

The length-scales σ_x and σ_t are learnable parameters indicating the variability of the function with regards to the hyperparameter input \mathbf{x} and number of training iterations t . Estimating appropriate values for them is critical as this represents the GPs prior regarding the sensitivity of performance w.r.t. changes in the number of training iterations and hyperparameters. For extremely large σ_t we expect the objective function to change very little for different numbers of training iterations. For small σ_t by contrast we expect drastic changes even for small differences.

We fit the GP hyperparameters by maximizing their posterior probability (MAP), $p(\sigma_x, \sigma_t | \mathbf{X}, \mathbf{t}, \mathbf{y}) \propto$

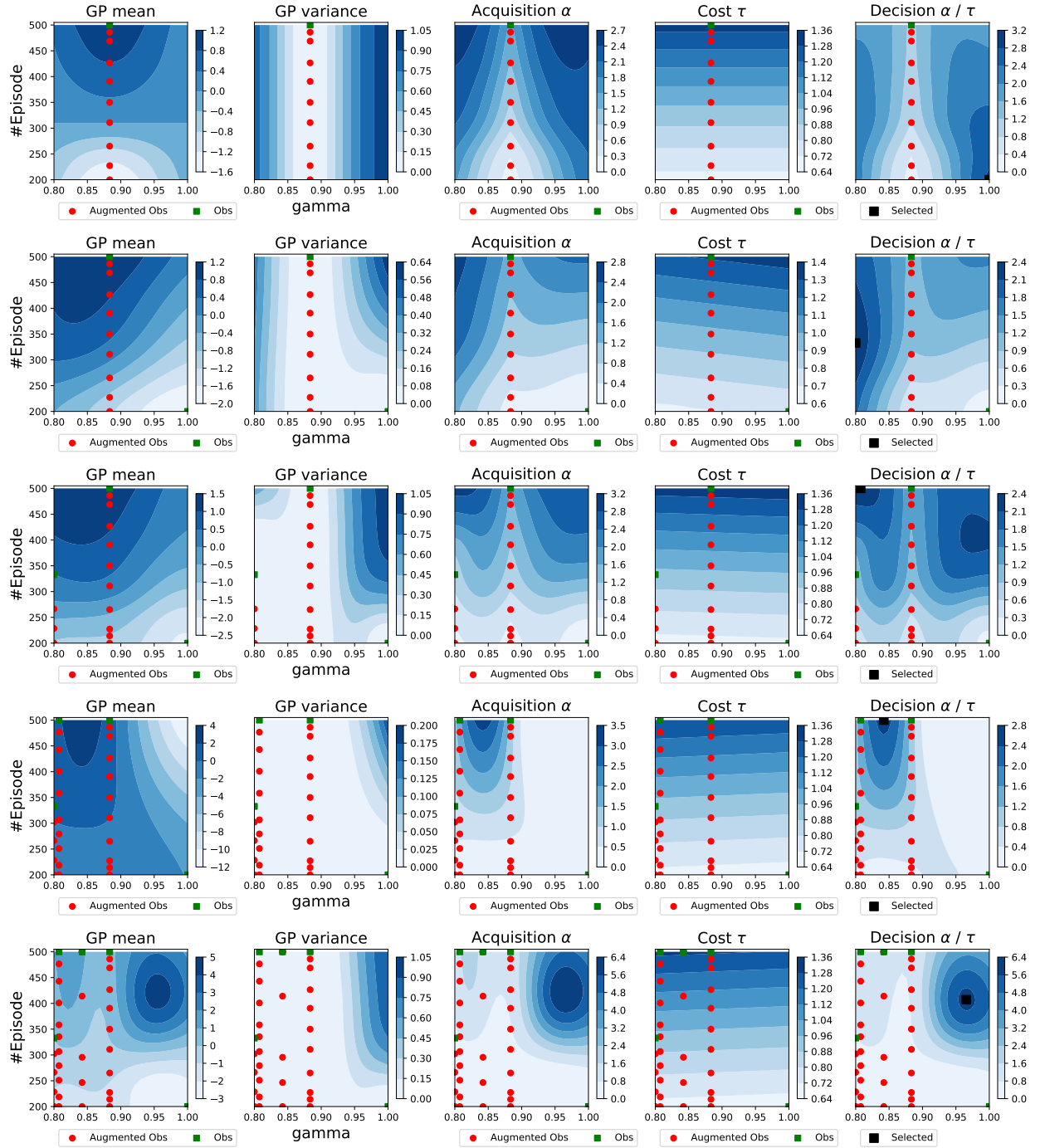


Figure 8: Illustration of BOIL on a 2-dimensional optimization task of DDQN on CartPole. The augmented observations fill the joint hyperparameter-iteration space quickly to inform our surrogate. Our decision balances utility α against cost τ for iteration-efficiency. Especially in situations of multiple locations sharing the same utility value, our algorithm prefers to select the cheapest option.

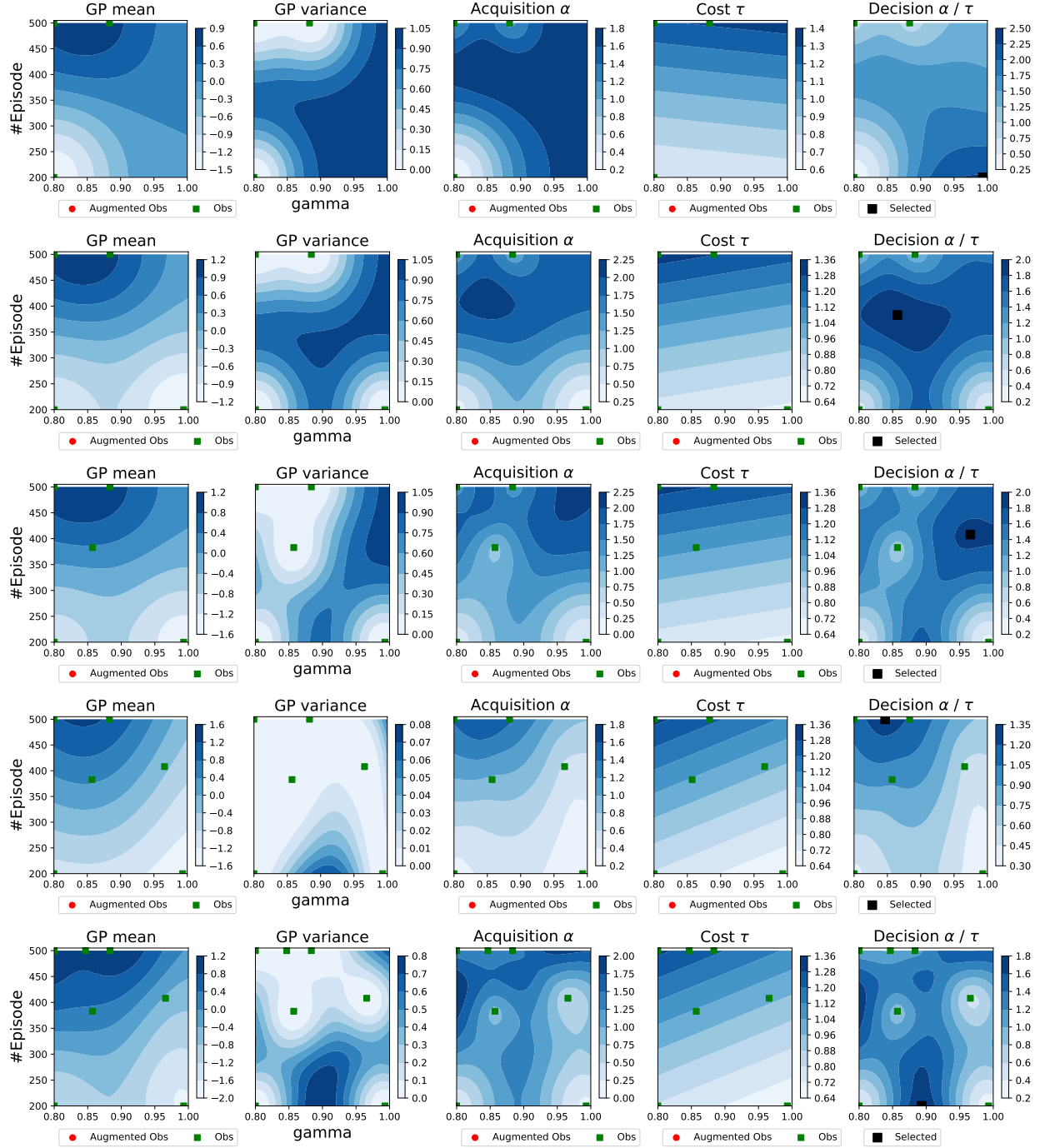


Figure 9: Illustration of the Continuous Multi-task BO (CMTBO) – this is the case of BOIL **without** using augmented observations (same setting as Fig. 8). This version leads to less efficient optimization for two main reasons. First, the additional iteration dimension requires more evaluation than optimizing the hyperparameters on their own. Second, the algorithm can reselect parameters at lower fidelity (less training iterations) despite having evaluated a higher fidelity already.

$p(\sigma_x, \sigma_t, \mathbf{X}, \mathbf{t}, \mathbf{y})$, which, thanks to the Gaussian likelihood, is available in closed form as (Rasmussen, 2006)

$$\ln p(\mathbf{y}, \mathbf{X}, \mathbf{t}, \sigma_x, \sigma_t) = -\frac{1}{2} \ln |K + \sigma^2 \mathbf{I}_N| - \frac{1}{2} \mathbf{y}^T (K + \sigma^2 \mathbf{I}_N)^{-1} \mathbf{y} + \ln p_{hyp}(\sigma_x, \sigma_t) + \text{const} \quad (10)$$

where \mathbf{I}_N is the identity matrix in dimension N (the number of points in the training set), and $p_{hyp}(\sigma_x, \sigma_t)$ is the prior over hyperparameters, described in the following.

We optimize Eq. (10) with a gradient-based optimizer, providing the analytical gradient to the algorithm. We start the optimization from the previous hyperparameter values θ_{prev} . If the optimization fails due to numerical issues, we keep the previous value of the hyperparameters. We refit the hyperparameters every $3 \times d$ function evaluations where d is the dimension.

Remark. Our focus in this paper is to demonstrate the effectiveness on optimizing the learning curve by compressing the curve into a value and augmenting the data for modeling efficiency. Therefore, we have not yet demonstrated the proposed model on various acquisition functions and kernel choices. However, other choices of kernels and acquisition functions are straightforward to be used in our model.

B Algorithm Illustration

Fig. 8 and Fig. 9 illustrate the behavior of our proposed algorithm BOIL on the example of optimizing the discount factor γ of Dueling DQN (Wang et al., 2016) on the CartPole problem. The two settings differ in the inclusion augmented observations into BOIL in Fig. 8 and CMTBO (or BOIL without augmented observations) in Fig. 9.

In both cases, we plot the GP predictive mean in Eq. (1), GP predictive variance in Eq. (2), the acquisition function in Eq. (3), the predicted function and the final decision function in Eq. (8).

As shown in the respective figures the final decision function balances between utility and cost of any pair (γ, t) to achieve iteration efficiency. Especially in situations where multiple locations share the same utility value, our decision will prefer to select the cheapest option. Using the augmented observations in Fig. 8, our joint space is filled quicker with points and the uncertainty (GP variance) across it reduces faster than in Fig. 9 – the case of vanilla CMTBO without augmenting observations. A second advantage of having augmented observations is that the algorithm is discouraged to select the same hyperparameter setting at lower fidelity than a previous evaluation. We do not add the full curve as this will make the conditioning problem of the GP covariance matrix.

Table 1: Dueling DQN algorithm on CartPole problem.

Variables	Min	Max	Best Parameter \mathbf{x}^*
γ discount factor	0.8	1	0.95586
learning rate model	$1e^{-6}$	0.01	0.00589
#Episodes	300	800	-

Table 2: A2C algorithm on Reacher problem.

Variables	Min	Max	Best Parameter \mathbf{x}^*
γ discount factor	0.8	1	0.8
learning rate actor	$1e^{-6}$	0.01	0.00071
learning rate critic	$1e^{-6}$	0.01	0.00042
#Episodes	200	500	-

B.1 Experiment settings

We summarize the hyper-parameter search ranges for A2C on Reacher in Table 2, A2C on InvertedPendulum in Table 3, CNN on SHVN in Table 4 and DDQN on CartPole in Table 1. Additionally, we present the best found parameter \mathbf{x}^* for these problems. Further details of the DRL agents are listed in Table 5.

B.2 Robustness over Different Preference Functions

We next study the learning effects with respect to different choices of the preference functions. We pick three preference functions including the Sigmoid, Log and Average to compute the utility score for each learning curve. Then, we report the best found reward curve under such choices. The experiments are tested using A2C on Reacher-v2. The results presented in Fig. 10 demonstrate the robustness of our model with the preference functions.

B.3 Examples of Deep Reinforcement Learning Training Curves

Finally, we present examples of training curves produced by the deep reinforcement learning algorithm A2C in Fig. 11. These fluctuate widely and it may not be trivial to define good stopping criteria as done for other applications in previous work (Swersky et al., 2014).

Table 3: A2C algorithm on InvertedPendulum problem.

Variables	Min	Max	Best Parameter \mathbf{x}^*
γ discount factor	0.8	1	0.95586
learning rate q model	$1e^{-6}$	0.01	0.00589
learning rate v model	$1e^{-6}$	0.01	0.00037
#Episodes	700	1500	-

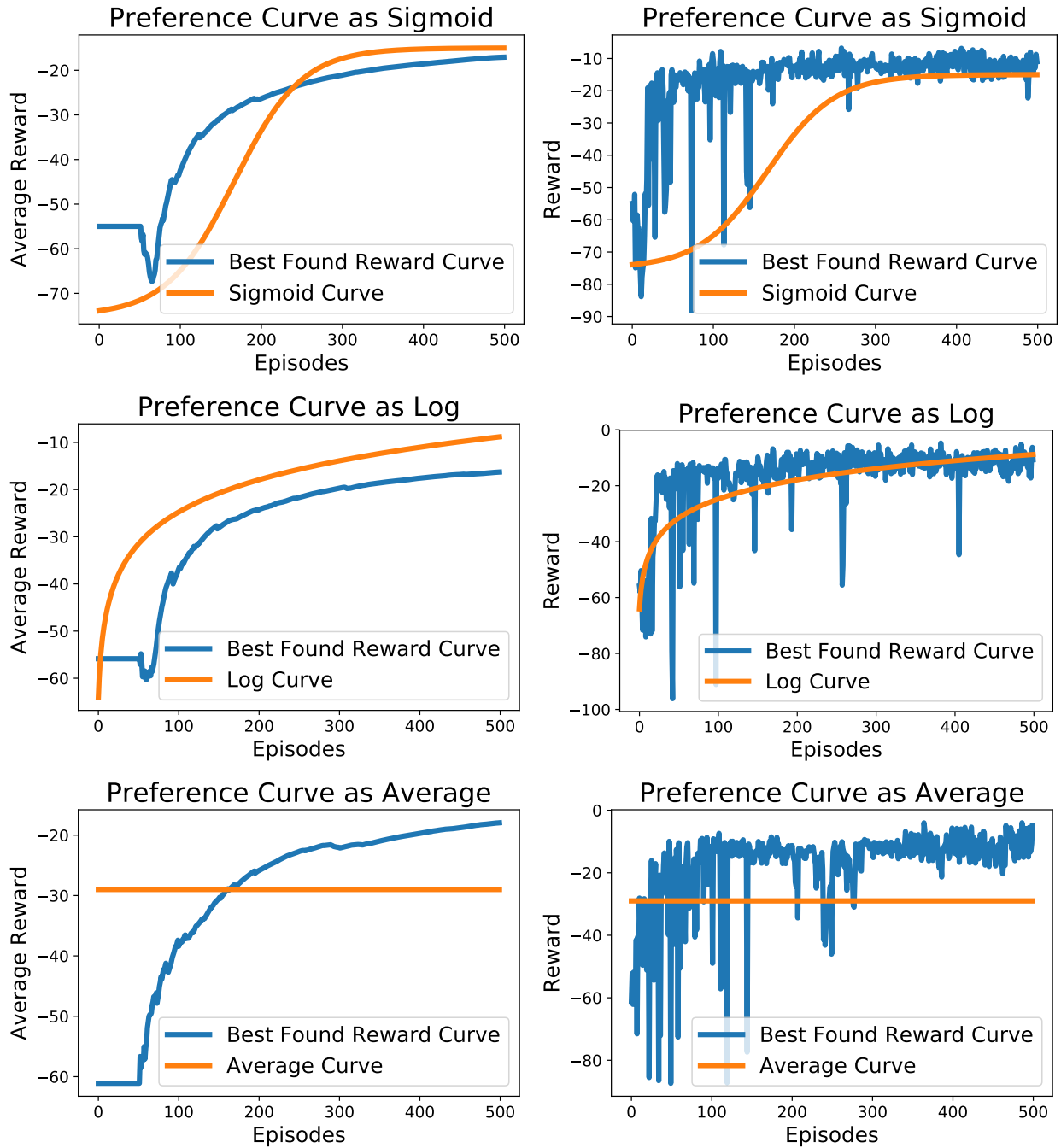


Figure 10: To highlight the robustness, we examine the results using different preference functions such as Sigmoid curve, Log curve, and Average curve on Reacher experiments. The results include the best found reward curve with different preference choices that show the robustness of our model.

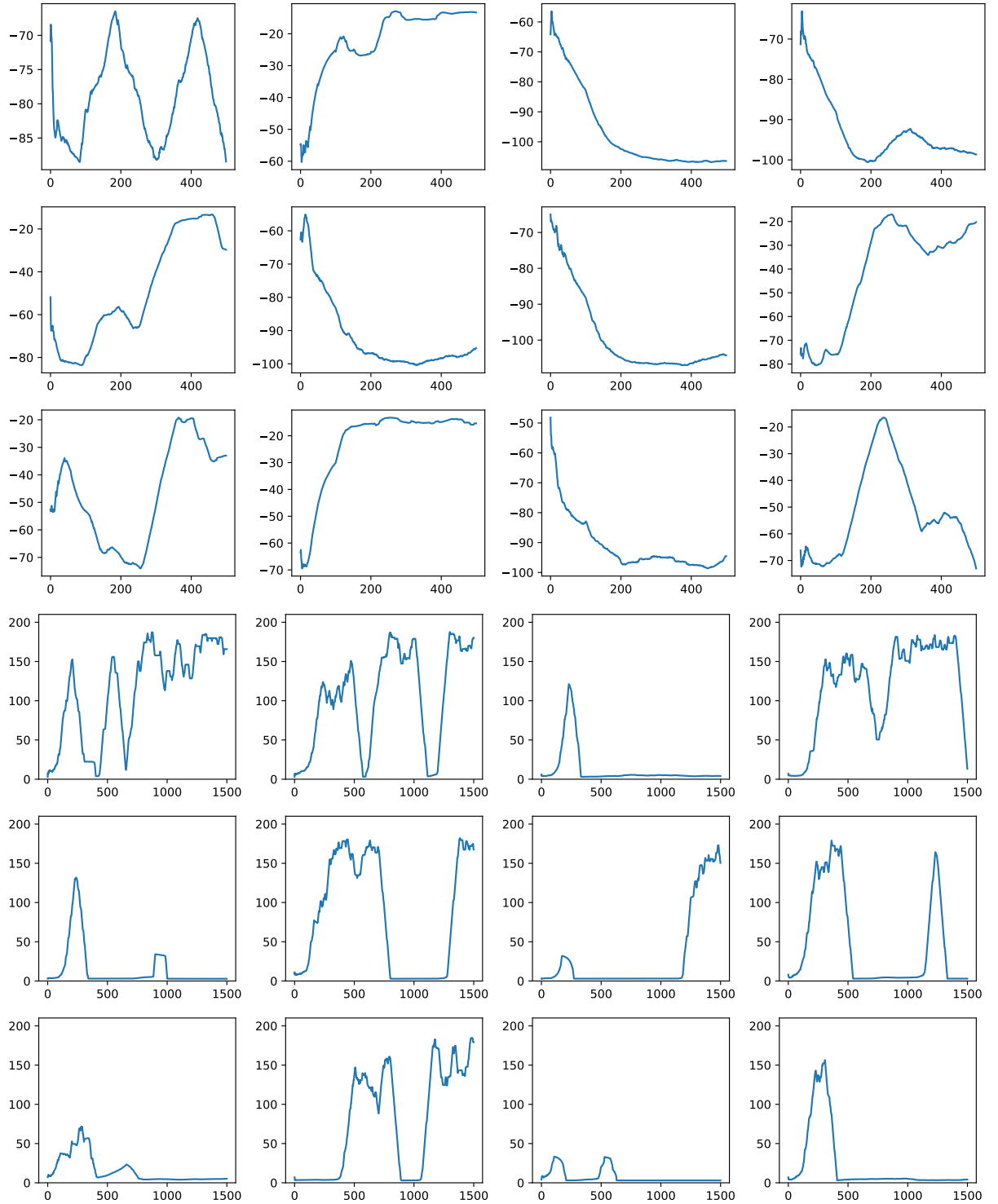


Figure 11: Examples of reward curves using A2C on Reacher-v2 (rows 1 – 3) and on InvertedPendulum-v2 (rows 4 – 6). Y-axis is the reward averaged over 100 consecutive episodes. X-axis is the episode. The noisy performance illustrated is typical of DRL settings and complicates the design of early stopping criteria. Due to the property of DRL, it is not trivial to decide when to stop the training curve. In addition, it will be misleading if we only take average over the last 100 iterations.

Table 4: Convolutional Neural Network on SVHN dataset.

Variables	Min	Max	Best Found \mathbf{x}^*
filter size	1	8	5
pool size	1	5	5
batch size	16	1000	8
learning rate	$1e^{-6}$	0.01	0.000484
momentum	0.8	0.999	0.82852
decay	0.9	0.999	0.9746
number of epoch	30	150	-

Table 5: Further specification for DRL agents

Hyperparameter	Value
A2C	
Critic-network architecture	[32,32]
Actor-network architecture	[32,32]
Entropy coefficient	0.01
Duelling DQN	
Q-network architecture	[50,50]
ϵ -greedy (start, final, number of steps)	(1.0, 0.05, 10000)
Buffer size	10000
Batch size	64
PER- α (Schaul et al., 2016)	1.0
PER- β (start, final, number of steps)	(1.0, 0.6, 1000)